Heliyon 10 (2024) e25322

Contents lists available at ScienceDirect

Heliyon

journal homepage: www.cell.com/heliyon

Research article

Differential responses of green-synthesized iron nano-complexes in mitigating bicarbonate stress in almond trees

Soosan Mohamadi [a], Soheil Karimi [a,**], Vahid Tavallali [b,*]

[a] Department of Horticultural Science, College of Aburaihan, University of Tehran, Tehran, Iran
[b] Department of Agriculture, Payame Noor University (PNU), P.O. Box: 19395-3697, Tehran, Iran

ARTICLE INFO

Keywords:
Hydrogen peroxide
Lime-induced chlorosis
Nanofertilizer
Proteins
Oxidative damage

ABSTRACT

High bicarbonate concentration in the soil induces iron (Fe) deficiency in fruit trees. According to the promising performance of nanomaterials in supplying mineral nutrients, in this study the potential of 4 green synthesized Fe nano-complexes (Fe–NCs) on alleviating bicarbonate stress in almond trees was evaluated in a soilless culture. The Fe–NCs were formed on extracts of husks of almond, pistachio, walnut, and pomegranate and their efficiency in Fe supply was compared to a commercial FeEDDHA fertilizer. The bicarbonate stress was imposed by adding sodium bicarbonate + calcium carbonate to the Hoagland's nutrient solution: Control (without sodium bicarbonate + calcium carbonate); 10 mM $NaHCO_3$+5 mM $CaCO_3$; 20 mM $NaHCO_3$+10 mM $CaCO_3$. The plants were irrigated with nutrient solutions containing different concentrations of bicarbonate and different sources of Fe for 120 days. Bicarbonate stress induced chlorophyll decline, proline accumulation and leaf necrosis, and decreased leaf area. These responses were in line with decline in Fe concentration and development of oxidative damage in leaves, as hydrogen peroxide accumulation and membrane stability index decline were observed in the bicarbonate-stressed plants. Although walnut-nFe and pistachio-nFe intensified these adverse effects of bicarbonate stress, the almond-nFe and pomegranate-nFe recovered chlorophyll concentration, alleviated the oxidative damage, and restored Fe in the plants to the range of FeEDDHA under bicarbonate stress. Alleviating the damages was related to retrieving the concentration of proteins, hydrogen peroxide detoxification, and catalase activity in the leaves. These findings uncovered the potential of green synthesized almond-nFe and pomegranate-nFe as low-cost and effective Fe sources under bicarbonate stress.

1. Introduction

Iron (Fe), as an essential micronutrient, is required for the health and functioning of the photosynthesis system of plant crops. In addition to chlorophyll biosynthesis and chloroplast health, electron transport in the chloroplast and mitochondria and the function of some enzymes are dependent on Fe supply [1]. Therefore, a shortage of physiologically active Fe lowers the efficiency of photosystem II Fv/Fm photochemistry and photosynthesis capacity of crops [2]. Moreover, Fe as the prosthetic group of antioxidant enzymes catalase and peroxidases involves in hydrogen peroxide detoxification in the cell [3]. Despite the important roles of Fe in cell function

* Corresponding author.
** Corresponding author.
E-mail addresses: skarimi@ut.ac.ir (S. Karimi), v.tavalali@pnu.ac.ir (V. Tavallali).

https://doi.org/10.1016/j.heliyon.2024.e25322
Received 17 August 2023; Received in revised form 28 November 2023; Accepted 24 January 2024
Available online 1 February 2024

and metabolism, Fe deficiency is a widespread nutritional disorder in plants [4]. Fe deficiency causes chlorosis and necrosis of young leaves which in severe conditions results in shoot dieback and decreased plant productivity [5,6]. Fe deficiency is associated with several edaphic factors, including high bicarbonate content, high pH, high redox potential, and low content of organic matter [7]. These conditions are dominant in the calcareous alkaline soils of arid and semi-arid areas [6] and the Fe deficiency disorder symptom in these soils is known as lime-induced chlorosis. The high concentration of bicarbonate in alkaline and calcareous soils prevents the Fe absorption by the root and its translocation to the shoot [8].

Bicarbonate can maintain a high pH (7.5–8.0) in the medium, due to its pH buffering capacity. This situation reduces Fe solubility in the soil and root Fe reductase activity which has an optimal pH of about 5.0 [9]. Bicarbonate can also induce iron chlorosis by alkalinizing the leaf apoplast, which reduces Fe III reduction and iron uptake by leaf mesophyll cells [10]. Bicarbonate stress probably by reduction of H^+ extrusion and the imbalance between C and N metabolisms prevents Fe translocation to shoots [9]. In addition to pH-mediated effects, bicarbonate can intensify the Fe deficiency by preventing the induction of Fe reductase activity in Fe-deficient Strategy I plants [11]. Fe-deficient plants are characterized by stunted growth and low productivity and interveinal chlorosis in the youngest leaves. Reduced yield and increased management costs are the consequences of Fe deficiency in calcareous alkaline soils [12].

The application of synthetic chelated fertilizers is of vital importance for supplying Fe in alkaline and calcareous soils [13]. FeEDDHA is the most successful Fe chelate that is currently the most widely used Fe fertilizer in agriculture [14]. High prices and low content of iron are the major disadvantages of this fertilizer [15]. Furthermore, potential toxicity to some species also may restrict their applicability [15,16]. Therefore, the investigation and development of new Fe sources are required for sustainable crop production in alkaline and calcareous soils [12].

The nanomaterials science is a novel window on the mineral nutrition of plant crops. Nanomaterials are increasingly used in agriculture and represent new ideas and directions for global crop production [17,18]. Nano fertilizers have shown the potential to increase the efficiency of mineral nutrients and provide mineral requirements of plants along with imparting sustainability to crop production systems [19]. The development of nanomaterials has led to the manufacturing of innovative agrochemicals and novel delivery mechanisms for promoting plant productivity and fertilizer use efficiency [20]. Studies have proved that the application of nano fertilizers minimizes the potential negative effects associated with overdosage, and reduces the frequency of fertilization [21,22]. Rui et al. [23] proved that Fe nanoparticles can successfully replace traditional chelated Fe fertilizers in peanut production. Liu et al. [24] showed that application of Fe nanoparticles significantly stimulated the growth of lettuce seedlings in hydroponics. Alidoust and Isoda [22] demonstrated that the phytotoxicity of Fe nanoparticles is lower than micro-sized fertilizers under reductive conditions. Other researches have also shown that the use of nanofertilizers has increased the plant's tolerance to the mineral nutrients stress and other environmental stressors [25]. By regulating the antioxidant enzyme system and levels of proline and phytohormones such as gibberellin-3, abscisic acid, zeatin riboside and indole-3-acetic acid, CeO_2 nanoparticles reduced oxidative membrane and DNA damage and increased plant tolerance to N stress [26]. Application of nanoparticles induces stress/immune responses by signaling and activating defense-related pathways, such as plant hormone signal transduction, glutathione metabolism, flavon and flavonol biosynthesis, MAPK signaling pathway, and plant-pathogen interaction. In this way, the application of nanoparticles not only stimulated germination of rice under stress conditions, but also increases the tolerance of seedlings against biotic and abiotic stresses [27]. Therefore, Fe nanomaterials have a high potential for achieving sustainable agriculture by enhancing production efficiency and minimizing damage to lands and water resources [19]. In an earlier study, we discovered that FeEDDHA and nano-Fe particles complexed with salicylic acid were equally effective at supplying plant requirements under bicarbonate and high pH stress. Additionally, the plants that received the Fe-NC demonstrated higher salinity tolerance, compared to plants treated with FeEDDHA, [12].

Complexing nanoparticles with organic compounds increase their stability and acquiring function. These compounds may have advantages such as increased stability/solubility, higher absorption or translocation, progressive release, and, in some cases, controlled delivery [28]. As a progressive step towards the development of greener and more sustainable systems, efforts have lately been undertaken to generate agrochemicals using food and agricultural by-products. The appeal of using wastes of food and fruit residues to lessen chemical use has increased. NCs have been synthesized using banana and tea wastes, grape and orange peels, orange and banana peels, papaya peels, and sugarcane bagasse [29,30]. The electrochemical and antibacterial characteristics of palladium, gold, and silver nanoparticles produced from *Cissus quadrangularis* stems were studied by Anjana et al. [31]. Behravan et al. [32] produced NCs via a green synthesis method using fruit peel waste. However, the characteristics of the generated NCs were strongly influenced by the type and composition of the organic matter used. Thousands of tons of waste are produced annually from pomegranate, pistachio, almond, and walnut husks that can be used in green synthesis of nanomaterials. These residues are a rich source of bioactive compounds such as flavonoids (anthocyanins, catechins, and other complex flavonoids), hydrolyzable tannins (pedunculagin, punicalin, punicalagin, and ellagic and gallic acids), and phenolic acids (hydroxycinnamic and hydroxybenzoic acids), which have been demonstrated to have high affinity to Fe [20,33–35]. Therefore, in the current study novel nano Fe complexes were synthesized from pomegranate, pistachio, almond, and walnut husks to develop inexpensive and environmentally friendly Fe sources to use in alkaline calcareous conditions. The effectiveness of these compounds in supplying Fe was compared with a commercial FeEDDHA fertilizer, by evaluating the growth, health, and performance of almond trees in a controlled environment. Stone fruits, including almond (*Prunus dulcis* Mill.), are sensitive Fe deficiency in calcareous alkaline soils [36]. Fe deficiency adversely affects growth and yield and increases management costs of stone fruits in arid and semi-arid regions, where bicarbonate stress is prevalent [37]. The production of novel and environmentally friendly fertilizers to supply Fe in bicarbonate-rich soils is an important management strategy to reduce the risk of environmental damage while increasing the productivity of plant crops.

2. Material and methods

2.1. Synthesis of Fe NC

Husks of pomegranate, walnut, pistachio, and almond were dried at 70 °C for 96 h. The dried husks were grinded to fine powders and separately extracted by distilled water at 60 °C for an hour. After being filtered with filter paper, the content of total phenols was measured in the samples and then, the extracts were utilized to green synthesis of Fe-NC. The total content of phenols in the extracts was determined by the Folin-Ciocalteu test. According to Sohrabi et al. [38]. The extracts were diluted in double distilled water (1:1, v: v) and 62.5 μL of Folin–Ciocalteu reagent was added to 62.5 μL of the diluted extracts. After 5 min, 125 μL of 0.1 M sodium carbonate and 1 mL of deionized water were added. The samples were kept in a dark room for 2 h and then centrifuged. The absorbance of the supernatants was measured at 760 nm using a spectrophotometer (PerkinElmer, Lambda 25, USA). The results were expressed as a mean of gallic acid equivalent.

In accordance with our most current research, 20 mL of each extract was mixed with 80 mL of 20 mM iron (III) chloride ($FeCl_3$) to synthesize green nano Fe with specific modifications [28]. Using an ultrasonic probe and sonication settings (amplitude of oscillation: 80 %; duration: 30 min), the mixes were sonicated. Each NC undergoes a color change in the reaction solution at this point, signifying the formation of a Fe-NC. Following centrifugation for 15 min at 3000 rpm, the products were separated and then they were continually washed with ethanol and deionized distilled water to remove impurities. The remaining ingredients were dried at 80 °C for 4 h. The dried Fe–NCs were grinded and fine powders were examined and characterized using Transmission Electron Microscopy (TEM) at 100 kV (Ziess, EM-900) and Attenuated Total Reflection - Fourier Transform Infrared Spectrophotometry (ATR-FTIR) (Tensor II).

2.2. Plant material and growing conditions

The plant material was two-year-old 'Shahroud-18′ almond trees grafted on bitter almond seedling rootstock. The trees were in pots containing a loamy soil. At the end of the growing season, uniform trees were selected for the experiment and defoliated by foliar application of zinc sulfate 5 % and transferred to cold storage (4 °C). After 30 days, the plants were removed from the pots. Their roots were completely washed off the soil, and the plants were transferred to large plastic pots (25 × 30 cm) containing 9 kg of washed sand + perlite (2:1 v/v). The plants were grown in a greenhouse with average temperatures of 32/25 day/night and relative humidity of 40 %. Fe-free Hoagland's nutrient solution with a 3-day interval was used for irrigation of the plants.

2.3. Treatments and the experimental design

Thirty days after the bud break, the plants were subjected to different concentrations of bicarbonate and different Fe sources in the nutrient solution. The bicarbonate was added to the nutrient solution as different concentrations of sodium bicarbonate + calcium carbonate. The treatments were Control (0.0 mM $NaHCO_3$ + 0.0 mM $CaCO_3$, pH = 7.1); 10 mM $NaHCO_3$ + 5 mM $CaCO_3$; and 20 mM $NaHCO_3$ + 10 mM $CaCO_3$. The bicarbonate-containing solutions had a pH of 8.1 ± 0.1. The Fe source treatments were Fe-free solution and four nano Fe NCs with different chelating agents (extract of the husk of walnut, pistachio, almond and pomegranate), and a FeEDDHA fertilizer (4.8 % [o-o]EDDHA chelated, Eurosolids®, Spain). In these treatments, Fe concentration was equal to the standard level of the Hoagland's solution (50 μM). The treatments were arranged as a factorial experiment based on a completely randomized block design with four replicates. 120 days after starting the treatments, the physiological and biochemical responses of the plants were investigated.

2.4. Measurement of parameters

2.4.1. Plant growth

Leaf area was measured by a leaf area meter (ADC Bioscientific, UK). The number of plant leaves and the number of necrosed leave were counted and the percentage of necrosed leaves were calculated. For measurement of specific leaf mass (SLM), 15 leaf discs with 5.0 mm diameter were dried at 70 °C for 72 h and their dry mass was measured. The SLM was calculated according to the following equation (Eq. 1).

$$SLM = Dry\ mass\ of\ leaf\ discs / Area\ of\ leaf\ discs \quad \text{Eq. 1}$$

2.4.2. Leaf chlorophyll concentration

Concentration of chlorophylls was determined in fully expanded young leaves on top of the shoot. Leaf samples were homogenized in 80 % acetone. After centrifugation, the extracts were brought to a final volume of 10 ml using 80 % acetone. Absorption of the samples was measured at 663.2 and 646.8 nm, and concentrations of the pigments were calculated using the formula developed by Lichtenthaler [39].

2.4.3. Membrane stability index

The plasma membrane stability index (MSI) was determined by measuring electrolyte leakage in fully expanded young leaves [40]. Twenty uniform leaf discs were floated in 10 ml deionized water and incubated at 40 °C for 30 min. After measuring their initial

electrical conductivity (C1), the samples were heated in boiling water for 10 min. The electrical conductivity was measured for the second time (C2) and the MSI was calculated using the following equation (Eq. 2):

$$MSI = 1 - \left(C1/C2\right) \times 100 \quad \text{Eq. 2}$$

2.4.4. Proline concentration in leaves

To measure proline, 500 mg of dried leaf samples were extracted in 3 % sulfosalicylic acid. After infiltration, to 2 ml of the filtered extract, 2 mL of acetic acid and 2 mL of ninhydrin acid reagent were added. The resulting solution was heated in boiling water bath for 1 h. The resulted chromophores were extracted with toluene and absorbance of the samples was measured using a spectrophotometer at 520 nm [41].

2.4.5. Oxidative damage indices

Hydrogen peroxide (H_2O_2) concentration in the leaves was determined according to the method developed by Velikova et al. [42]. Leaf tissue was extracted with cold trichloroacetic acid (TCA) in potassium phosphate buffer. After centrifuging, KI was added to the samples. The light absorbance of the samples was measured at 390 nm by spectrophotometry (PerkinElmer, Lambda 25, USA).

Leaf samples were homogenized in cold TCA to quantify malondialdehyde (MDA) concentration in leaves. After centrifugation, the supernatants were mixed with thiobarbituric acid in 20 % TCA. The samples were heated in a boiling water bath for 30 min and the absorbance of the samples was measured at 532 and 600 nm using a spectrophotometer (PerkinElmer, Lambda 25, USA). The MDA concentration was calculated using an extinction coefficient of 155 mM cm^{-1} after withdrawing the non-specific absorbance at 600 nm [43].

2.4.6. Concentration of proteins and catalase activity in leaves

For measurement of total protein concentration and activity of the antioxidant enzyme, catalase, 1 g of leaf tissue was homogenized in 50 mM sodium phosphate buffer. After centrifuging at 12 kg at 4 °C, the concentration of proteins in the supernatant was determined according to the method developed by Bradford [44]. Catalase activity also was determined in the prepared samples according to the method described in Cakmak and Marschner [45].

2.4.7. Fe content of leaves

Leaf samples were washed with a regular dishwashing liquid, and rinsed with deionized water. The leaves were oven-dried at 70 °C for 70 h and then ground to obtain a fine powder. The samples were ashed in an electric furnace and analyzed for total Fe by atomic absorption spectrometry (Agilent 240 AA, Agilent Technologies, USA). The data were expressed as Fe concentration per dry mass of leaves and Fe content in leaves of the plants.

2.5. Statistical analyses

The treatments were arranged as a factorial experiment (6 Fe treatments × 3 bicarbonate treatments) based on a completely

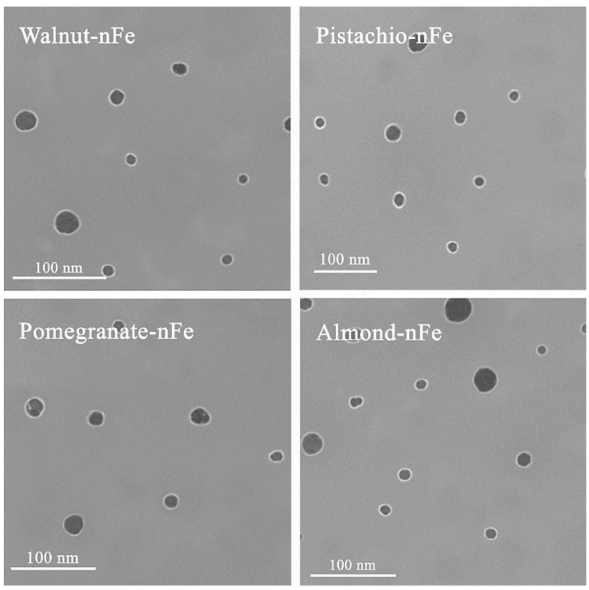

Fig. 1. Transmission electron micrographs of the nano-Fe complexes used in this study.

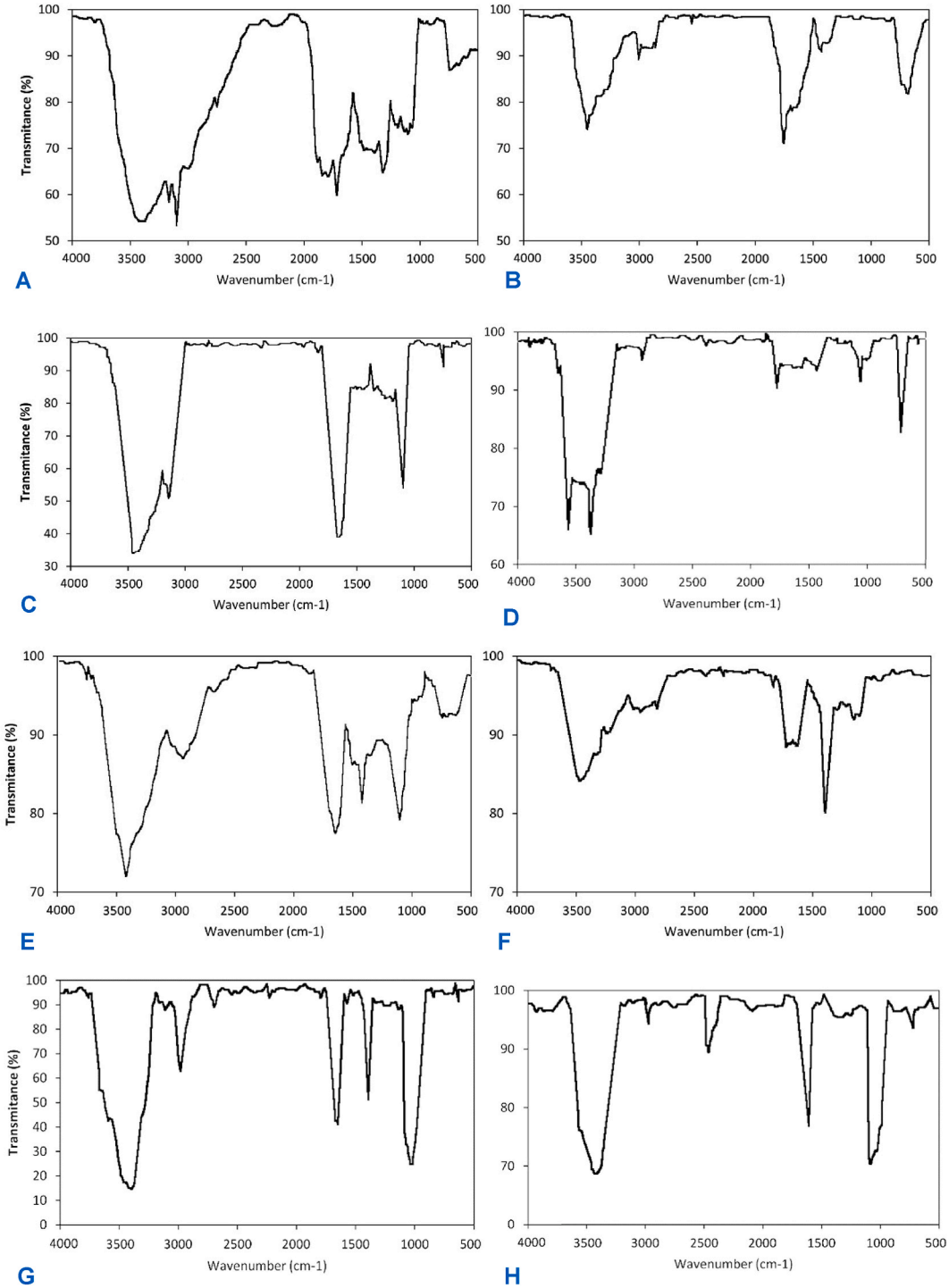

Fig. 2. FT-IR spectra of husk extracts of almond (A), pistachio (C), walnut (E) and pomegranate (G) and FT-IR spectra of green synthetic Fe-NC from husk extracts of almond (B), pistachio (D), walnut (F), and pomegranate (H).

randomized block design with four replications. In sum, 72 plants were used in this experiment. After an analysis of variance (ANOVA), the means were separated by Duncan's multiple range test (DMRT) at $P \leq 0.05$. Data analyses were performed by SPSS v 21.0 software.

3. Results

The formation of nano Fe complexes was investigated by taking transmission electron micrographs at 100 kV and the Fourier transform infrared spectroscopy (FT-IR). Transmission electron microscopy confirmed the formation of Fe complexes at the nanoscale (Fig. 1). The size of the nano-complexes was between 10 and 25 nm.

Fig. 2A and b represent the FT-IR spectra of the green synthetic Fe-NC and almond husk extract, respectively. Stretching bands at 3421 cm^{-1} are observed in the FTIR spectrum of the almond husk extract (Fig. 2A) for OH functional groups like alcohols, phenols, and carboxylic acids. Saturated hydrocarbons (Csp 3-H), carbonyl group (C]O) stretching, C]C aromatic ring stretching, C–O stretching, aromatic, C–H out of plane bending, and O–H out of plane bending vibrations, respectively, are related to absorption bands at 2926 and 2855, 1608, 1698, and 1457, 1216, 1073, 826, and 771 cm^{-1}. Fig. 2B displays the synthesized Fe NC's FTIR spectrum. It demonstrates that multifunctional groups are present on the Fe-NC surface. As a result of biomolecules capping onto the surface of NC, this suggests that almond husk extract plays a significant role in the reducing and stabilizing of Fe NC. However, the interaction between Fe and the phytochemical active sites in the almond husk extract for the production of NC results in a variation in the shape and shift of the absorption bands.

Fig. 2c and d represent the FT-IR spectrum of the Fe-NC that was synthesized using pistachio husk extract. According to the FT-IR spectrum for Fe NC, surface hydroxyls and coupled pistachio husk extract molecules were found on Fe. Both the strong peak at 3370 cm^{-1} and the peak at 3570 cm^{-1} are caused by the O–H group that is free from hydrogen bonds. The presence of molecules from pistachio husk extract in the synthesized iron nano-complex was shown by the peaks at 3305 and 3370 cm^{-1}. In contrast to the FT-IR spectrum of pure pistachio husk extract, the band at 1012 cm^{-1} is due to the C–O stretching vibration organizing to iron metal cations. Fig. 2C suggests that hydrogen bonds may have formed between the molecules of the pistachio husk extract and the iron components. The alkyl chains in the pistachio husk extract are thought to be responsible for the absorption bands at 2815 and 2915 cm^{-1}. The hydrogen-bonded hydroxyl groups and the bending mode of the hydroxyl group in water are responsible for the peaks at 3305 cm^{-1} and 1623 cm^{-1}. The Fe–OH bond is seen by the peak at 1407 cm^{-1}. The Fe–OH vibrations are indicated by the peak at 1013 cm^{-1}. The Fe–*O*–H bond is responsible for the peaks that were seen at 416 cm^{-1} to 932 cm^{-1}. These variations show that the pistachio husk extract functions as a capping and dispersing agent for an artificial iron nano-complex.

The FT-IR spectra of the green synthesized Fe-NC and the husk extract of walnut were similar to one another, as shown in Fig. 2e and f, and alterations were seen in the peaks' magnitude and quantity. The OH functional groups of alcohols and phenolic compounds may be responsible for the two different peaks at 3413 cm^{-1} and 3410 cm^{-1}. The observed peaks at 2926 cm^{-1} and 2927 cm^{-1} might be due to alkanes spanning from C to H. Fe-NC spectra had a peak at 1707 cm^{-1}, which was likely caused by C]O stretching. There are two distinct peaks at 1564 cm^{-1} and 1601 cm^{-1} that are connected to the vibration of C]C stretching and the frequency of C]O stretching, respectively. The two distinct peaks at 1369 cm^{-1} and 1401 cm^{-1} might be the result of C–H deformation and Fe-NC binding to the carboxylate and hydroxyl groups of various protein residues, respectively. In the Fe-NC spectra, a peak at 1054 cm^{-1} that was present in the extract spectrum was split into two peaks at 1082 cm^{-1} and 1049 cm^{-1}. The C–O vibrational frequency, the N–C bond stretching of aliphatic amine groups, and the C-stretching of ether groups were each attributed to them. The extract spectrum's faint peak at 930 cm^{-1} was likely caused by alkene groups being stretched along the C–H axis. In the Fe-NC spectra, a peak at 878 cm^{-1} that was present in the extract spectrum was split into two peaks at 872 cm^{-1} and 834 cm^{-1}. The 834 cm-peak may correlate to the in-plane and out-of-plane bending of the benzene ring, while the 878 cm^{-1} peak may be related to the stretching vibration of carbohydrate. We could wrap up by saying that any biomolecule that has these linkages can function as a reducing or capping agent.

Fig. 2G displays the FT-IR spectra of pomegranate husk extract. The FT-IR spectrum's several peaks revealed the complexity of system. N–H stretching of amides, carboxylic acid - OH stretch, and alcohol/phenol - OH stretching vibration, all exhibit a strong broad

Table 1
Effects of Fe sources and bicarbonate concentrations in the nutrient solution on the growth indices and chlorophylls' concentration in leaves of almond trees.

	Plant leaf area (cm^2)	Necrosed leaves (%)	Specific leaf mass (g/m^2)	Chlorophylls (μg/g FM)
Fe Source				
-Fe	1607.2 ± 171.7^{c}	6.95 ± 1.06^{a}	4.26 ± 0.16^{d}	1236.6 ± 111.8^{c}
Walnut-nFe	1537.7 ± 150.7^{c}	4.39 ± 0.78^{ab}	9.22 ± 0.45^{b}	1619.7 ± 82.2^{a}
Pistachio-nFe	1694.4 ± 147.9^{b}	5.30 ± 1.33^{ab}	7.06 ± 0.96^{c}	1524.7 ± 78.4^{b}
Pomegranate-nFe	2002.3 ± 262.0^{a}	0.00 ± 0.00^{c}	8.60 ± 0.84^{bc}	1603.8 ± 103.4^{a}
Almond-nFe	1888.9 ± 134.2^{ab}	2.39 ± 0.72^{bc}	12.98 ± 1.00^{a}	1598.3 ± 67.6^{a}
FeEDDHA	1884.4 ± 218.8^{ab}	3.85 ± 1.24^{b}	11.93 ± 0.96^{a}	1616.0 ± 94.7^{a}
HCO_3^- (mM)				
0	2268.9 ± 111.8^{a}	0.00 ± 0.00^{c}	8.23 ± 0.93^{a}	2001.3 ± 65.5^{a}
10	1889.3 ± 67.6^{b}	2.00 ± 0.41^{b}	8.55 ± 0.63^{a}	1677.3 ± 80.4^{b}
20	1163.8 ± 91.5^{c}	12.39 ± 1.07^{a}	9.45 ± 0.87^{a}	977.5 ± 105.4^{c}

Means ($n = 4$) ± standard errors marked by the same letters are not statistically different according to DMRT at $P \leq 0.05$.

absorption band at 3411 cm^{-1}. The stretching mode of CH_3 and CH_2 can be used to explain absorption bands at 2938 cm^{-1}. The C]O stretching in the carboxyl groups or the C]N bending in the amide groups may be responsible for the strong peaks at 1742 cm^{-1}. Primary amines with an NH stretch are characteristic of the peak at 1623 cm^{-1}. Peaks at 1526 cm^{-1}, 1460 cm^{-1}, 1364 cm^{-1}, and 1233 cm^{-1} are identified by C–C–N amines, aromatic –CH stretching vibrations, and NH in secondary amines. The sharp peak at 1064 cm^{-1} implied the (NH)–C–O group's stretching vibration. Peaks at 900-526 cm^{-1} refer to C–N–C, N–C]O, and O–C]O bending mines in carboxylic acids. The prominent band at 431 cm^{-1} in the FT-IR spectra of synthetic Fe NC, shown in Fig. 2H and is attributable to the vibrations of extension and bending of vibratory Fe. Water being absorbed on the surface of Fe-NC is what causes the intense absorption peak at 3446 cm^{-1}, which is related to the O–H stretching mode. The structural alterations in the FT-IR spectra showed that the coordination with OH, –NH, C]O, and C]N helped to cap and stabilize the iron nano-complex. Pomegranate husk extract's physicochemical characteristics serve as a capping agent and stop the generated nano-complex from aggregating.

The rate of recovery of polyphenols from the extracts of husks of almond, pistachio, walnut, or pomegranate fruits was 146.8, 32.4, 103.0, and 365.2 mg gallic acid/g dried material, respectively. Details on ANOVA results can be found in the supplemental data attached to the paper. The effects of Fe source and bicarbonate treatments were significant on leaf area and percentage of necrosed leaves. The Fe-deficient plants and walnut-Fe-NC received plants had the lowest leaf area. The highest leaf area was observed in pomegranate-nFe received plants, which was statistically similar to that in the almond-nFe and FeEDDHA treated plants (Table 1). Increasing bicarbonate concentration in the nutrient solution, significantly reduced plant leaf area. The plants in the control treatment (0 mM bicarbonate) had the highest leaf area. The lowest leaf area was found under the 20 mM bicarbonate stress condition (Table 1).

The Fe-deficient plants had the highest percentage of necrosed leaves which was statistically similar to that in the walnut-nFe, or

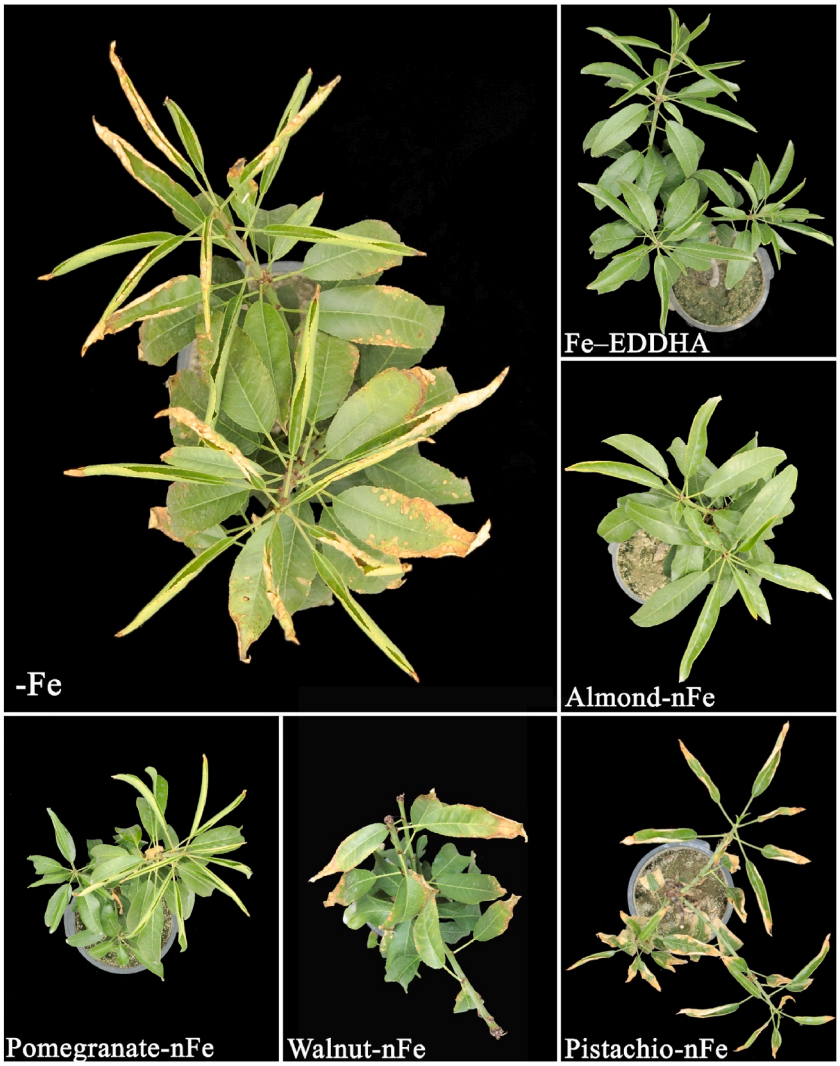

Fig. 3. Visual comparison of the almond trees in response to Fe deficiency and application of plant based nano Fe complexes under severe bicarbonate stress and high pH stress in the Hoagland's nutrient solution. Application of almond-nFe and pomegranate-nFe complexes were as effective as FeEDDHA in alleviating adverse effects of sodium bicarbonate stress.

pistachio-nFe received plants. The lowest frequency of necrosed leaves was observed in the pomegranate-nFe received plants, which was statistically equal to that in the almond-nFe treated plants (Table 1). The percentage of necrosed leaves increased with increasing concentration of bicarbonate in the nutrient solution. The plants in the control treatment (0 mM bicarbonate) had no necrosed leaves, and those under the 20 mM bicarbonate stress had the highest percentage of necrosed leaves (Table 1). Fig. 3 visually compares the almond trees treated with different Fe sources under 20 mM bicarbonate stress in the nutrient solution.

The effect of the Fe source was significant on the SLM. The Fe-deficient plants had the lowest SLM and the application of Fe in the nutrient solution significantly increased SLM. The highest SLM was found in the almond-nFe and the FeEDDHA-received plants (Table 1). The effects of Fe source and bicarbonate treatments were significant on total chlorophyll concentration in the leaves. The Fe-deficient plants had the lowest concentration of chlorophylls in their leaves. The application of Fe significantly increased the concentration of chlorophylls in the young fully expanded leaves. Among the Fe complexes, pistachio-nFe resulted in a lower chlorophyll concentration in the leaves (Table 1). Increasing bicarbonate concentration in the nutrient solution significantly decreased chlorophyll concentration in the leaves. The plants in the control treatment (0 mM bicarbonate) had the highest chlorophyll concentration in their leaves. The lowest chlorophyll concentration was found under the 20 mM bicarbonate stress condition (Table 1).

The effects of the Fe source, bicarbonate concentration and their interaction were significant on MSI and proline concentration in the leaves. According to the interactive effect of the treatments (Fig. 4A), the lowest MSI was found in the Fe-deficient plants under the bicarbonate stress conditions. Fe application significantly increased MSI in the leaves. The highest MSI was observed in the Fe-received plants in the absence of bicarbonate stress and no significant differences were found between different Fe sources. Increasing bicarbonate concentration in the nutrient solution decreased MSI in the leaves of Fe-received plants. Under the 20 mM bicarbonate stress, the highest MSI was found in leaves of FeEDDHA-treated plants, which was statistically similar to that in the almond-nFe received plants.

Increasing the concentration of bicarbonate in the nutrient solution increased the concentration of proline in the leaves of the Fe-deficient plants, and the plants treated with pistachio-nFe and FeEDDHA. The highest proline concentration was found in leaves of Fe-deficient plants and the plants treated with pistachio-nFe and FeEDDHA received plants under 20 mM bicarbonate stress. In almond-nFe and pomegranate-nFe received plants, no significant change in leaf proline concentration was observed under different levels of bicarbonate (Fig. 4B).

The effect of bicarbonate stress was significant on the leaf hydrogen peroxide concentration. Hydrogen peroxide concentration in leaves of plants under 10 mM bicarbonate was similar to that in the control treatment. The application of 20 mM bicarbonate stress in the nutrient solution significantly increased hydrogen peroxide concentration in the leaves (Table 2). The effect of Fe source or application of bicarbonate in the nutrient solution on MDA was not significant.

The effects of the Fe source and bicarbonate stress treatments were significant on the concentration of proteins and CAT activity in the leaves. The concentration of proteins in leaves of the Fe-deficient plants was significantly lower than the Fe received plants (Table 2). The control plants without the bicarbonate application had the highest concentration of proteins. The application of

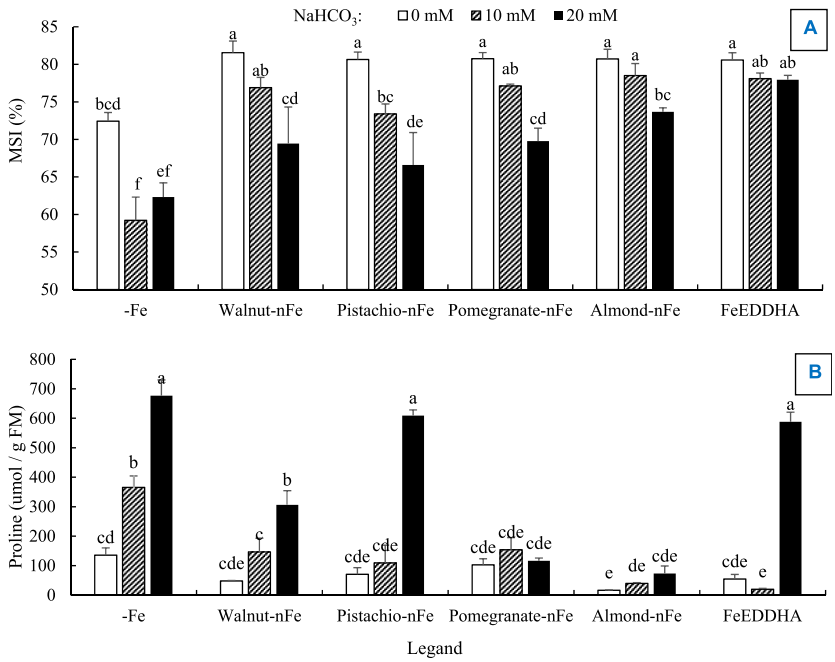

Fig. 4. Interactive effects of Fe sources × bicarbonate concentrations in the Hoagland's nutrient solution on A) membrane stability index (MSI) and B) proline concentration in leaves of almond trees. Means ($n = 4$) ± standard errors marked by the same letters are not statistically different according to DMRT at $P \leq 0.05$. The bars represent the standard errors of the means.

Table 2
Effects of Fe sources and bicarbonate concentrations in the nutrient solution on concentrations of proteins and hydrogen peroxide (H_2O_2), and catalase activity in leaves of almond trees.

	H_2O_2 (μmol/g FM)	Proteins (mg/g FM)	Catalase activity (Unit/min./mg Protein)
Fe Source			
-Fe	36.0 ± 2.2[a]	6.14 ± 0.38[b]	2.23 ± 1.06[c]
Walnut-nFe	31.0 ± 2.0[a]	6.69 ± 0.15[a]	7.33 ± 0.90[a]
Pistachio-nFe	34.0 ± 1.7[a]	6.65 ± 0.15[a]	5.26 ± 1.20[b]
Pomegranate-nFe	33.0 ± 2.3[a]	7.04 ± 0.14[a]	5.70 ± 1.00[ab]
Almond-nFe	31.2 ± 3.3[a]	6.65 ± 0.15[a]	7.27 ± 0.53[a]
FeEDDHA	32.4 ± 2.6[a]	6.73 ± 0.13[a]	6.54 ± 1.40[a]
HCO_3^- (mM)			
0	32.1 ± 1.6[b]	6.90 ± 0.10[a]	6.35 ± 1.20[a]
10	30.1 ± 1.5[b]	6.70 ± 0.11[ab]	6.69 ± 0.90[a]
20	37.8 ± 2.5[a]	6.50 ± 0.22[b]	4.62 ± 0.50[b]

Means ($n = 4$) ± standard errors marked by the same letters are not statistically different according to DMRT at $P \leq 0.05$.

bicarbonate in the nutrient solution decreased concentration of proteins in the leaves and the plants under 20 mM bicarbonate stress had the lowest concentration of proteins (Table 2). The Fe-deficient plants exhibited the lowest CAT activity in their leaves. Application of Fe significantly increased CAT activity in the leaves. Among the Fe treatments, pistachio-nFe treated plants exhibited the lowest CAT activity (Table 2). The highest CAT activity was found in 0 and 10 mM bicarbonate treatments. Application of 20 mM bicarbonate in the nutrient solution significantly decreased CAT activity in the leaves (Table 2).

The effects of Fe source, bicarbonate stress, and their interaction were significant on leaf Fe concentration and total Fe content in plant leaves. Investigating the interactive effect of the treatments indicated that under Fe deficiency condition, the concentration of Fe decreased with the application of bicarbonate in the nutrient solution; however, no significant difference was found between 10 and 20 mM bicarbonate treatments (Fig. 5A). Application of different Fe sources (except for walnut-nFe) significantly increased Fe concentration in leaves of the plants in comparison with the control treatment. By increasing the bicarbonate concentration in the nutrient solution, leaf Fe concentration increased in the Fe-received plants. The highest Fe concentration was found in leaves of almond-nFe treated plants under 20 mM bicarbonate stress. (Fig. 5A).

The interaction of Fe source and bicarbonate stress indicated that Fe-deficient trees had the lowest Fe content in the leaves. The highest Fe content was found in pomegranate-nFe treated plants without bicarbonate stress. Bicarbonate application did not affect Fe content in the leaves of plants in the Fe deficiency treatments (Fig. 5B). However, Fe content in the Fe NC-received plants decreased under bicarbonate stress treatments. Application of 20 mM bicarbonate and pistachio-nFe reduced the Fe content of leaves to the level

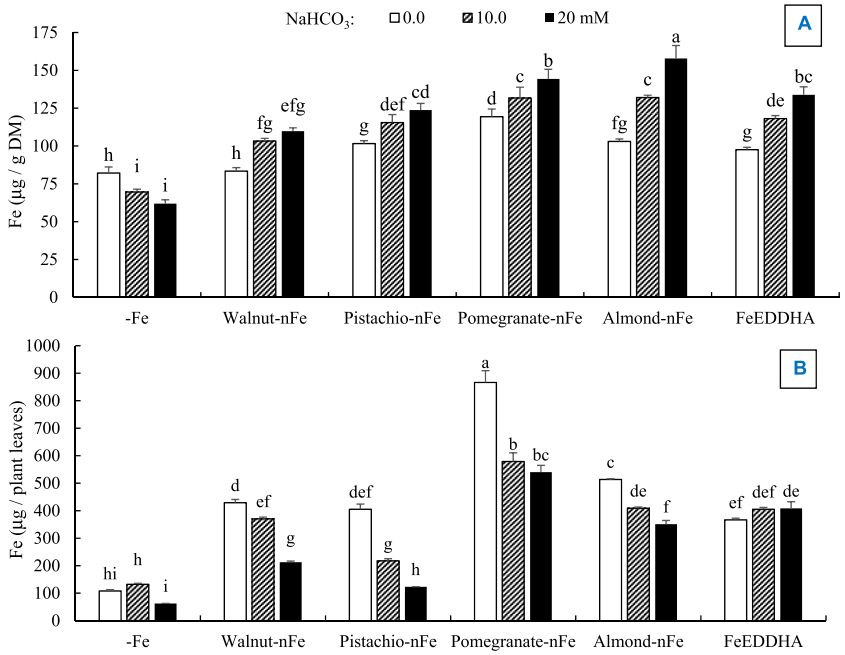

Fig. 5. Interactive effects of Fe sources × bicarbonate concentrations in the Hoagland's nutrient solution on A) leaf Fe concentration and B) Fe content in leaves of almond trees. Means ($n = 4$) ± standard errors marked by the same letters are not statistically different according to DMRT at $P \leq 0.05$. The bars represent the standard errors of the means.

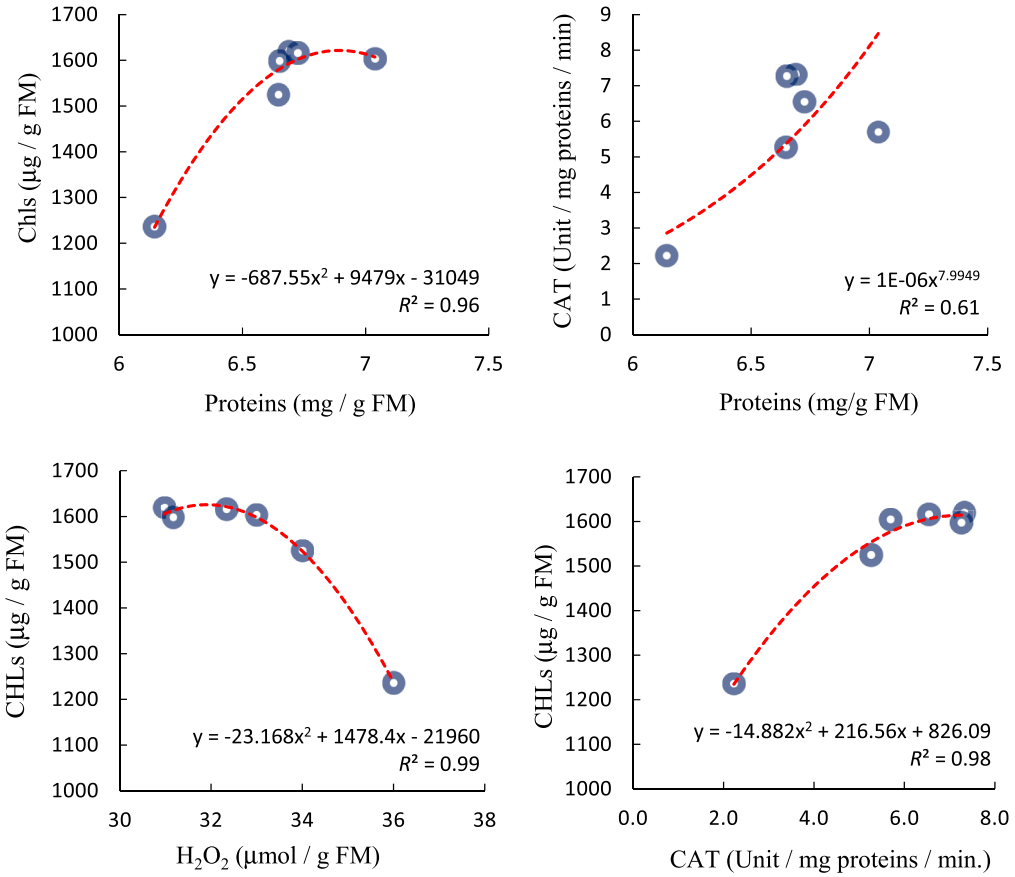

Fig. 6. Correlations of leaf proteins' concentration with chlorophylls' concentration and catalase activity (CAT) and correlations of leaf chlorophyll concentration with hydrogen peroxide (H_2O_2) concentration and catalase activity (CAT) in almond leaves under different Fe sources and bicarbonate concentrations in the Hoagland's nutrient solution.

of Fe-deficient plants. In the FeEDDHA received plants, the application of bicarbonate did not affect the Fe content of the leaves (Fig. 5B).

Fig. 6 represents the relationships between total chlorophylls and proteins concentration, hydrogen peroxide content and CAT activity in the leaves. Accordingly, chlorophyll content was positively correlated with protein content and CAT activity in the leaves. On the other hand, leaf chlorophylls declined with hydrogen peroxide accumulation in the leaves. A positive correlation was found between protein content and CAT activity in the leaves (Fig. 6).

4. Discussion

Fe deficiency and bicarbonate stress decreased SLM and leaf area and increased the frequency of necrotic leaves. Stunted growth due to bicarbonate stress, high pH, and Fe deficiency has been previously reported in other plant species [46–48]. Bicarbonate stress and Fe deficiency may restrict cell division and growth [49,50] by limitation of stomatal conductance, photosynthesis rate, photosystem II efficiency [49], restriction of the activity of stromal enzymes and prevention of formation of thylakoid membranes in the chloroplasts [51]. Therefore Fe deficiency-induced growth limitation appears to be a result of reduced photosynthesis activity. In agreement, the decrease in SLM confirmed that the photosynthesis activity of the plants was restricted under bicarbonate stress. SLM is directly related to leaf thickness, cell division, accumulation of reserve carbohydrates in the leaves [52], carbon assimilation rate and plant vigor [52,53]. The decrease in the SLM in the current study could be a result of chlorophyll decline and oxidative damage of leaves under Fe deficiency and bicarbonate stress conditions. Similar results were also reported by Tagliavini et al. [54] and Kong et al. [55].

In addition to the decrease in the photosynthetic area, the decline in the chlorophyll content of leaves decreased the photosynthetic capacity of the plants under Fe deficiency and bicarbonate stress conditions [56]. Chouliaras et al., [57] and Pestana et al., [58] also observed chlorophyll decline with increasing bicarbonate concentration and pH in the nutrient solution. The decline in the chlorophylls could be related to decreased availability of active Fe under bicarbonate stress [3], which decreases protein biosynthesis and inhibits chlorophyll biosynthesis by lowering δ-aminolevulinic acid and protochlorophyllide formation [3,59]. Moreover, accumulation of reactive oxygen species in the chloroplasts and decrease in antioxidative enzymes (catalase) induce chlorophyll degradation

and intensify the chlorophyll decline in the leaves under Fe deficiency situations. Therefore, Fe deficiency by damaging the photosynthetic apparatus limits carbon dioxide fixation [60,61]. Preservation of chlorophylls in the leaves is an indicator of plant tolerance to high pH and bicarbonate stress [46,47,51].

Contrary to the development of leaf chlorosis, the bicarbonate stressed plants had higher concentrations of Fe in their leaves. Similar observations have been reported by Toselli et al., [62] and Marschner [3]. Therefore it was concluded that bicarbonate induced leaf chlorosis by inactivation of Fe in the plants. Additionally, part of the increase in Fe in the leaves was due to leaf growth inhibition and the concentration effect [62]. The calculation of the total content of Fe in the leaves showed that increasing the bicarbonate ion in the nutrient solution is also effective in reducing Fe absorption. The results are in agreement with Nikolic and Römheld [10] who reported that absorption and translocation of Fe from roots to leaves of grape vine was reduced under bicarbonate stress.

Accumulation of hydrogen peroxide and leaf damages (MSI decline, proline accumulation and development of necrotic leaves) were observed under Fe deficiency and bicarbonate stress. Proline accumulation in the leaves with increasing concentration of bicarbonate in the nutrient solution also reflected the bicarbonate stress damage on almond trees. Previously, accumulation of proline and other amino acids were reported under iron deficiency stress conditions [63]. Proline accumulation in plants is a common defense response to environmental stress [25,64]. As an osmolyte and nitrogen source, proline protects the plant under environmental stress conditions and its accumulation is in line with the intensity of stress [65]. The accumulation of this amino acid can be caused by the reduction of protein biosynthesis and the direction of nitrogen towards the synthesis of this compound [3]. Therefore, the reduction of proline concentration in the leaves of plants under bicarbonate stress with Fe nutrition indicated the alleviation of bicarbonate stress pressure and the restoration of protein biosynthesis in plants. The effects of hydrogen peroxide accumulation on the cell membrane and chloroplast damage have been described in detail in the literature [66,67]. At least part of chlorophyll decline under these conditions was due to oxidative damage [3,68] In the current study, chlorophyll concentration was directly correlated with CAT activity (Fig. 6). The decrease in CAT activity under Fe deficiency and bicarbonate stress coincided with the depletion of protein concentration in the leave (Fig. 6) which resulted in the accumulation of hydrogen peroxide and oxidative damage. As the prosthetic group of antioxidant enzymes CAT and peroxidases, Fe involves in the detoxification of reactive oxygen species [47]. CAT detoxifies hydrogen peroxide and converts it to water [69,70]. The results indicated that the activity of this enzyme was governed by Fe supply to plants. Leaf proteins play a critical role in supporting and protecting photosynthetic pigments and preserving the integrity of the chloroplasts [71,72]. The majority of leaf proteins accumulate in the chloroplasts in association with chlorophylls [3]. Therefore, protein depletion in the cell triggers chlorophyll instability and degradation [3]. The protein biosynthesis limitations under Fe deficiency conditions have been related to the role of Fe in the structure, stability, and function of the ribosomes [73]. Therefore, the Fe NCs which increased the protein content of leaves were more effective in increasing the chlorophyll concentration (Fig. 6).

Application of the Fe NCs increased Fe concentration in the leaves and recovered the growth and health of almond trees under bicarbonate and high pH stresses. Many studies have demonstrated that nano Fe particles are more efficient than chelated Fe fertilizers in supplying Fe to plants [18,23]. In the current study, we observed that the organic ligand of the Fe-NC complexes significantly influenced the efficiency of the compounds in supplying Fe and alleviating the adverse effects of bicarbonate stress. Such differences also can be found among commercial chelated Fe fertilizers with different ligands [74,75]. Among the synthesized Fe NCs, pomegranate-nFe and almond-nFe were more efficient than pistachio-nFe or walnut-nFe. According to the total phenolics contents of the primary extracts of the fruit, the higher efficiency of almond-nFe and pomegranate-nFe could be due to the higher concentrations of phenols in their extracts.

On the other hand, the allelopathic activity of walnut and pistachio extracts could be the reason for the increased sensitivity of the plants to the bicarbonate stress conditions. The allelopathic effects of juglone in the leaf and green husk of walnut fruit are well documented in the literature [76]. Alyousef and Ibrahim [77] also showed that extracts of fruit and leaf of pistachio have substantial adverse effects on seed germination and seedling growth of other plants. Our results suggested that the allelopathic effects of the plant extracts may intensify the negative effects of severe bicarbonate stress. Therefore, the allelopathic activities of plants should be considered before using phyto-phenolics for the development of agrochemicals.

5. Conclusion

The results of this study uncovered the potential of phyto-phenolics recovered from crop wastes in synthesizing chelated nano Fe fertilizers. Pomegranate-nFe or almond-nFe compounds were as effective as FeEDDHA in improving the performance and health of almond trees under bicarbonate stress. However, it was concluded that the potential for adverse allelopathic activity of plants should be considered before using them in the development of plan-based chelated nano-fertilizers. The results uncovered the potential of Fe NCs as a strategy for the prevention or remedy of Fe chlorosis in alkaline and calcareous soils.

Data availability

Data will be made available on request.

CRediT authorship contribution statement

Soosan Mohamadi: Software, Resources, Methodology. **Soheil Karimi:** Writing – review & editing, Writing – original draft, Conceptualization. **Vahid Tavallali:** Supervision, Project administration, Methodology.

Declaration of competing interest

The authors declare that they have no known competing financial interests or personal relationships that could have appeared to influence the work reported in this paper.

Appendix A. Supplementary data

Supplementary data to this article can be found online at https://doi.org/10.1016/j.heliyon.2024.e25322.

References

[1] M. Broadley, P. Brown, I. Cakmak, Z. Rengel, F. Zhao, Function of nutrients: micronutrients, in: Marschner's Mineral Nutrition of Higher Plants, Elsevier Ltd, California, 2011, pp. 191–248, https://doi.org/10.1016/B978-0-12-384905-2.00007-8.

[2] P. Marschner, Marschner's Mineral Nutrition of Higher Plants, Academic press, 2011, https://doi.org/10.1016/B978-0-12-384905-2.00012-1.

[3] J. Zhao, W. Zhang, Q. Qiu, F. Meng, M. Zhang, D. Rao, Z. Wang, X. Yan, Physiological regulation associated with differential tolerance to iron deficiency in soybean, Crop Sci. 58 (3) (2018) 1349–1359.

[4] J.F. Briat, C. Dubos, F. Gaymard, Iron nutrition, biomass production, and plant product quality, Trends Plant Sci. 20 (1) (2015) 33–40.

[5] A.M. Liesch, D.A.R. Diaz, K.L. Martin, B.L. Olson, D.B. Mengel, K.L. Roozeboom, Management strategies for increasing soybean yield on soils susceptible to iron deficiency, Agron. J. 103 (2011) 1870–1877, https://doi.org/10.2134/agronj2011.0191.

[6] W.D.C. Schenkeveld, E.J.M. Temminghoff, A.M. Reichwein, W.H. van Riemsdijk, FeEDDHA-facilitated Fe uptake in relation to the behaviour of FeEDDHA components in the soil-plant system as a function of time and dosage, Plant Soil 332 (2011) 69–85, https://doi.org/10.1007/s11104-009-0274-9.

[7] E. Neubauer, W.D.C. Schenkeveld, K.L. Plathe, C. Rentenberger, F. von der Kammer, S.M. Kraemer, T. Hofmann, The influence of pH on iron speciation in podzol extracts: iron complexes with natural organic matter, and iron mineral nanoparticles, Sci. Total Environ. 461–462 (2013) 108–116, https://doi.org/10.1016/j.scitotenv.2013.04.076.

[8] F. Shahsavandi, S. Eshghi, A. Gharaghani, R. Ghasemi-Fasaei, M. Jafarinia, Effects of bicarbonate induced iron chlorosis on photosynthesis apparatus in grapevine, Sci. Hortic. 270 (2020) 109427, https://doi.org/10.1016/j.scienta.2020.109427.

[9] N. Wang, X. Dong, Y. Chen, B. Ma, C. Yao, F. Ma, Z. Liu, Direct and bicarbonate-induced iron deficiency differently affect iron translocation in Kiwifruit roots, Plants 9 (11) (2020) 1578, https://doi.org/10.3390/plants9111578.

[10] M. Nikolic, V. Römheld, Does high bicarbonate supply to roots change availability of iron in the leaf apoplast? Plant Soil 241 (1) (2002) 67–74, https://doi.org/10.1023/A:1016029024374.

[11] C. Lucena, F.J. Romera, C.L. Rojas, M.J. García, E. Alcántara, R. Pérez-Vicente, Bicarbonate blocks the expression of several genes involved in the physiological responses to Fe deficiency of Strategy I plants, Funct. Plant Biol. 34 (11) (2007) 1002–1009, https://doi.org/10.1071/FP07136.

[12] S. Karimi, V. Tavallali, L. Ferguson, S. Mirzaei, Developing a nano-Fe complex to supply iron and improve salinity tolerance of pistachio under calcium bicarbonate stress, Commun. Soil Sci. Plant Anal. 51 (14) (2020) 1835–1851, https://doi.org/10.1080/00103624.2020.1798985.

[13] A. Mann, A.L. Singh, Sh Oza, N. Goswami, D. Mehta, V. Chaudhari, Effect of iron source on iron deficiency induced chlorosis in groundnut, Legume Res. 40 (2) (2015) 241–249, https://doi.org/10.18805/lr.v0iOF.6849.

[14] L.M. Bin, L. Weng, M.H. Bugter, Effectiveness of FeEDDHA, FeEDDHMA, and FeHBED in preventing iron-deficiency chlorosis in soybean, J. Agric. Food Chem. 64 (44) (2016) 8273–8281.

[15] T.K. Broschat, K.K. Moore, Phytotoxicity of several iron fertilizers and their effects on Fe, Mn, Zn, Cu, and P content of african marigolds and zonal geraniums, Hortscience 39 (3) (2004) 595–598.

[16] J.P. Albano, D.J. Merhaut, Influence of FeEDDS, FeEDTA, FeDTPA, FeEDDHA, and FeSO4 on marigold growth and nutrition, and substrate and runoff chemistry, Hortscience 47 (1) (2012) 93–97, https://doi.org/10.21273/HORTSCI.47.1.93.

[17] S. Huang, L. Wang, L. Liu, Y. Hou, L. Li, Nanotechnology in agriculture, livestock, and aquaculture in China. A review, Agron. Sustain. Dev. 35 (2014) 369e400.

[18] A.D. Servin, J.C. White, Nanotechnology in agriculture: next steps for understanding engineered nanoparticle exposure and risk, NanoImpact 1 (2016) 9e12.

[19] T.B. Pirzadah, B. Malik, I. Tahir, K.R. Hakeem, H.F. Alharby, R.U. Rehman, Lead toxicity alters the antioxidant defense machinery and modulate the biomarkers in Tartary buckwheat plants, Int. Biodeterior. Biodegrad. 151 (2020) 104992, https://doi.org/10.1016/j.ibiod.2020.104992.

[20] V. Tavallali, S. Karimi, Green synthesized zinc-glycine chelate enhances antioxidant protection of pistachio under different soil boron levels, Int. J. Fruit Sci. 17 (4) (2017) 423–439, https://doi.org/10.1080/15538362.2017.1354246.

[21] G. Ghodake, Y.D. Seo, D.S. Lee, Hazardous phytotoxic nature of cobalt and zinc oxide nanoparticles assessed using Allium cepa, J. Hazard Mater. 186 (1) (2011) 952–955.

[22] D. Alidoust, A. Isoda, Phytotoxicity assessment of γ-Fe_2O_3 nanoparticles on root elongation and growth of rice plant, Environ. Earth Sci. 71 (2013) 5173–5182, https://doi.org/10.1007/s12665-013-2920-z.

[23] M. Rui, C. Ma, Y. Hao, J. Guo, Y. Rui, X. Tang, Q. Zhao, X. Fan, Z. Zhang, T. Hou, S. Zhu, Iron oxide nanoparticles as a potential iron fertilizer for peanut (Arachis hypogaea), Front. Plant Sci. 7 (2016) 815, https://doi.org/10.3389/fpls.2016.00815.

[24] R. Liu, H. Zhang, R. Lal, Effects of stabilized nanoparticles of copper, zinc, manganese, and iron oxides in low concentrations on lettuce (Lactuca sativa) seed germination: nanotoxicants or Nanonutrients? Water, Air, Soil Pollut. 227 (2016) 1–14, https://doi.org/10.2134/agronj2011.0191.

[25] Y. Wang, L. Wang, C. Ma, K. Wang, Y. Hao, Q. Chen, Y. Mo, Y. Rui, Effects of cerium oxide on rice seedlings as affected by co-exposure of cadmium and salt, Environ. Pol. 252 (2019) 1087–1096.

[26] Y. Wang, P. Zhang, M. Li, Z. Guo, S. Ullah, Y. Rui, I. Lynch, Alleviation of nitrogen stress in rice (*Oryza sativa*) by ceria nanoparticles, Environ. Sci.: Nano 7 (10) (2020) 2930–2940.

[27] X. Yan, S. Chen, Z. Pan, W. Zhao, Y. Rui, L. Zhao, AgNPs-triggered seed metabolic and transcriptional reprogramming enhanced rice salt tolerance and blast resistance, ACS Nano 17 (1) (2022) 492–504, https://doi.org/10.1021/acsnano.2c09181.

[28] V. Tavallali, V. Rowshan, H. Gholami, Sh Hojati, Iron-urea nano-complex improves bioactive compounds in essential oils of Ocimum basilicum L, Sci. Hortic. 265 (2020) 109222, https://doi.org/10.1016/j.scienta.2020.109222.

[29] M. Skiba, V. Vorobyova, Green synthesis of silver nanoparticles using grape pomace extract prepared by plasma-chemical assisted extraction method, Mol. Cryst. Liq. Cryst. 674 (1) (2018) 142–151.

[30] M.I. Skiba, V.I. Vorobyova, Synthesis of silver nanoparticles using orange peel extract prepared by plasmochemical extraction method and degradation of methylene blue under solar irradiation, Adv. Mater. Sci. Eng. 2019 (2019) 8306015.

[31] P.M. Anjana, M.R. Bindhu, R.B. Rakhi, Green synthesized gold nanoparticle dispersed porous carbon composites for electrochemical energy storage, Materials Science for Energy Technologies 2 (3) (2019) 389–395.

[32] M. Behravan, A.H. Panahi, A. Naghizadeh, M. Ziaee, R. Mahdavi, A. Mirzapour, Facile green synthesis of silver nanoparticles using Berberis vulgaris leaf and root aqueous extract and its antibacterial activity, Int. J. Biol. Macromol. 124 (2019) 148–154.

[33] A.M. Awwad, B. Albiss, Biosynthesis of colloidal copper hydroxide nanowires using Pistachio leaf extract, Adv. Mater. Lett. 6 (1) (2015) 51–54, https://doi.org/10.5185/amlett.2015.5630.

[34] Z. Abbasi, Sh Feizi, E. Taghipour, P. Ghadam, Green synthesis of silver nanoparticles using aqueous extract of dried Juglans regia green husk and examination of its biological properties, Green Process. Synth. 6 (2017) 477–485, https://doi.org/10.1515/gps-2016-0108.

[35] A. Bahmanzadegan, H. Tavallali, V. Tavallali, M.A. Karimi, Variations in biochemical characteristics of Zataria multiflora in response to foliar application of zinc nano complex formed on pomace extract of Punica granatum, Ind. Crops Prod. 187 (2022) 115369.

[36] A.J. Felipe, *Felinem, garnem* and *monegro* Almond×Peach hybrid rootstocks, Hortscience 44 (1) (2009) 196–197.

[37] M. Sanz, J. Cavero, J. Abadía, Iron chlorosis in the Ebro river basin, Spain, J. Plant Nutr. 15 (10) (1992) 1971–1981, https://doi.org/10.1080/01904169209364451.

[38] M. Sohrabi, M.Z. Mehrjerdi, S. Karimi, V. Tavallali, Using gypsum, selenium foliar application for mineral biofortification and improving the bioactive compounds of garlic ecotypes, Ind. Crop. Prod. 154 (2020) 112742, https://doi.org/10.1016/j.indcrop.2020.112742.

[39] H.K. Lichtenthaler, Chlorophyll and carotenoids: pigments of photosynthetic biomembranes, Methods Enzymol. 148 (1987) 350–382.

[40] A. Blum, A. Ebercon, Cell membrane stability as a measure of drought and heat tolerance in wheat, Crop Sci. 21 (1981) 43–47, https://doi.org/10.2135/cropsci1981.0011183X002100010013x.

[41] L.S. Bates, R.A. Waldren, I.D. Teare, Rapid determination of free proline for water-stress studies, Plant Soil 39 (1973) 205–207, https://doi.org/10.1007/BF00018060.

[42] V. Velikova, I. Yordanov, A. Edreva, Oxidative stress and some antioxidant system in acid rain treated bean plants: protective role of exogenous polyamines, Plant Sci. 151 (2000) 59–66, https://doi.org/10.1016/S0168-9452(99)00197-1.

[43] R.L. Heath, L. Packer, Photoperoxidation in isolated chloroplasts. I. Kinetics and stochiometry of fatty acid peroxidation, Arch. Biochem. Biophys. 125 (1968) 189–198, https://doi.org/10.1016/0003-9861(68)90654-1.

[44] M.M. Bradford, A rapid and sensitive method for the quantitation of microgram quantities of protein utilizing the principle of protein-dye binding, Anal. Biochem. 72 (1976) 248–254, https://doi.org/10.1016/0003-2697(76)90527-3.

[45] I. Cakmak, H. Marschner, Magnesium deficiency and high light intensity enhance activities of superoxide dismutase, ascorbate peroxidase, and glutathione reductase in bean leaves, Plant Physiol. 98 (4) (1992) 1222–1227, https://doi.org/10.1104/pp.98.4.1222.

[46] C. Ma, J.C. White, J. Zhao, Q. Zhao, B. Xing, Uptake of engineered nanoparticles by food crops: characterization, mechanisms, and implications, Annu. Rev. Food Sci. Technol. 9 (2018) 129–153, https://doi.org/10.1146/annurev-food-030117-012657.

[47] W. Msehli, M. DellOrto, P. De Nisi, S. Donnini, C. Abdelly, G. Zocchi, M. Gharsalli, Responses of two ecotypes of Medicago ciliaris to direct and bicarbonate-induced iron deficiency conditions, Acta Physiol. Plant. 31 (4) (2009) 667–673, https://doi.org/10.1007/s11738-009-0288-1.

[48] M. Incesu, T. Yesiloglu, B. Cimen, B. Yilmaz, C. Akpinar, I. Ortas, Effects on growth of persimmon (Diospyros virginiana) rootstock of arbuscular mycorrhizal fungi species, Turk. J. Agric. For. 39 (2015) 117–122, https://doi.org/10.3906/tar-1405-134.

[49] L. Bavaresco, M. Bertamini, F. Iacono, Lime-induced chlorosis and physiological responses in grapevine (Vitis vinifera L. cv. Pinot blanc) leaves, Vitis 45 (1) (2006) 45–46.

[50] F. Šrámek, M. Dubský, Occurrence and correction of lime-induced chlorosis in petunia plants, Plant Soil Environ. 57 (4) (2011) 180–185.

[51] V. Chouliaras, K. Dimassi, I. Therios, A. Molassiotis, G. Diamantidis, Root-reducing capacity, rhizosphere acidification, peroxidase and catalase activities and nutrient levels of Citrus taiwanica and C. volkameriana seedlings, under Fe deprivation conditions, Agronomie 24 (2004) 1–6, https://doi.org/10.1051/agro:2003055.

[52] K. Jumrani, V.S. Bhatia, G.P. Pandey, Impact of elevated temperatures on specific leaf weight, stomatal density, photosynthesis and chlorophyll fluorescence in soybean, Photosynth. Res. 131 (3) (2017) 333–350, https://doi.org/10.1007/s11120-016-0326-y.

[53] L. Xi, L. Yong, Varietal difference in the correlation between leaf nitrogen content and photosynthesis in rice (Oryza sativa L.) plants is related to specific leaf weight, J. Integr. Agric. 15 (9) (2016) 2002–2011, https://doi.org/10.1016/S2095-3119(15)61262-X.

[54] M. Tagliavini, D. Bassi, B. Marangoni, Growth and mineral nutrition of pear rootstocks in lime soils, Sci. Hortic. 54 (1) (1993) 13–22, https://doi.org/10.1016/0304-4238(93)90079-6.

[55] W.L. Kong, X.Q. Wu, Y.J. Zhao, Effects of Rahnella aquatilis JZ-GX1 on treat chlorosis induced by iron deficiency in Cinnamomum camphora, J. Plant Growth Regul. 39 (2019) 877–887, https://doi.org/10.1007/s00344-019-10029-8.

[56] M.D. De La Guardia, E. Alcántara, A comparison of ferric-chelate reductase and chlorophyll and growth ratios as indices of selection of quince, pear and olive genotypes under iron deficiency stress, Plant Soil 241 (1) (2002) 49–56, https://doi.org/10.1023/A:1016083512158.

[57] V. Chouliaras, I. Therios, A. Molassiotis, G. Diamantidis, Iron chlorosis in grafted sweet orange (*Citrus sinensis* L.) plants: physiological and biochemical responses, Biol. Plant. (Prague) 48 (1) (2004) 141–144, https://doi.org/10.1023/B:BIOP.0000024292.51938.aa.

[58] M. Pestana, P. Beja, P.J. Correia, A. De Varennes, E.A. Faria, Relationships between nutrient composition of flowers and fruit quality in orange trees grown in calcareous soil, Tree Physiol. 25 (2005) 761–767, https://doi.org/10.1093/treephys/25.6.761.

[59] A. Molassiotis, V. Panteli, E. Patiraki, et al., Complementary and alternative medicine use in lung cancer patients in eight European countries, Compl. Ther. Clin. Pract. 12 (2006) 34–39.

[60] B. Cimen, T. Yesiloglu, M. Incesu, B. Yilmaz, Growth and photosynthetic response of young 'Navelina' trees budded on to eight citrus rootstocks in response to iron deficiency, N. Z. J. Crop Hortic. Sci. 42 (3) (2014) 170–182, https://doi.org/10.1080/01140671.2014.885064.

[61] O. Sahin, A. Gunes, M.B. Taskin, A. Inal, Investigation of responses of some apple (Mallus × domestica Borkh.) cultivars grafted on MM106 and M9 rootstocks to lime-induced chlorosis and oxidative stress, Sci. Hortic. 219 (2017) 79–89, https://doi.org/10.1016/j.scienta.2017.03.006.

[62] M. Toselli, B. Marangoni, M. Tagliavini, Iron content in vegetative, reproductive organs of nectarine trees in calcareous soils during the development of chlorosis, Eur. J. Agron. 13 (2000) 279–286, https://doi.org/10.1016/S1161-0301(00)00065-4.

[63] C. Arias-Baldrich, N. Bosch, D. Begines, A.B. Feria, J.A. Monreal, S. García-Mauriño, Proline synthesis in barley under iron deficiency and salinity, J. Plant Physiol. 183 (2015) 121–129.

[64] S. Karimi, Z. Mirfattahi, L. Ferguson, V. Tavallali, Using controlled salt stress and β-aminobutyric acid signaling to decrease transplant failure, Sci. Hortic. 225 (2017) 156–162, https://doi.org/10.1016/j.scienta.2017.06.070.

[65] S. Karimi, F. Ehterami-Fini, Comparing different pretreatments at transplanting stage for acclimation of walnut trees to hot and dry conditions, Plant Stress 2 (2021) 100036, https://doi.org/10.1016/j.stress.2021.100036.

[66] M.C. Dias, S. Correia, J. Serôdio, A.M.S. Silva, H. Freitas, C. Santos, Chlorophyll fluorescence and oxidative stress endpoints to discriminate olive cultivars tolerance to drought and heat episodes, Sci. Hortic. 231 (2018) 31–35, https://doi.org/10.1016/j.scienta.2017.12.007.

[67] L.-T. Dinis, A.C. Malheiro, A. Luzio, H. Fraga, H. Ferreira, I. Gonçalves, G. Pinto, C.M. Correia, J. Moutinho-Pereira, Improvement of grapevine physiology and yield under summer stress by kaolin-foliar application: water relations, photosynthesis and oxidative damage, Photosynthetica 56 (2) (2018) 641–651, https://doi.org/10.1007/s11099-017-0714-3.

[68] M. Valipour, B. Baninasab, A.H. Khoshgoftarmanesh, M. Gholami, Oxidative stress and antioxidant responses to direct and bicarbonate-induced iron deficiency in two quince rootstocks, Sci. Hortic. 261 (2020) 108933, https://doi.org/10.1016/j.scienta.2019.108933.

[69] J. Zhang, H. Li, B. Xu, J. Li, B. Huang, Exogenous melatonin suppresses dark-induced leaf senescence by activating the superoxide dismutase-catalase antioxidant pathway and down-regulating chlorophyll degradation in excised leaves of perennial ryegrass (Lolium perenne L.), Front. Plant Sci. 7 (2016) 1500, https://doi.org/10.3389/fpls.2016.01500.

[70] M.N. Alyemeni, M.A. Ahanger, L. Wijaya, P. Alam, R. Bhardwaj, P. Ahmad, Selenium mitigates cadmium-induced oxidative stress in tomato (Solanum lycopersicum L.) plants by modulating chlorophyll fluorescence, osmolyte accumulation, and antioxidant system, Protoplasma 255 (2) (2018) 459–469, https://doi.org/10.1007/s00709-018-1231-3.

[71] M. Yamada, R. Nagao, M. Iwai, Y. Arai, A. Makita, H. Ohta, T. Tomo, The PsbQ' protein affects the redox potential of the Q A in photosystem II, Photosynthetica 56 (1) (2018) 185–191, https://doi.org/10.1007/s11099-018-0778-8.

[72] E. Kuthanová Trsková, D. Bína, S. Santabarbara, R. Sobotka, R. Kaňa, E. Belgio, Isolation and characterization of CAC antenna proteins and photosystem I supercomplex from the cryptophytic alga Rhodomonas salina, Physiol. Plantarum 166 (1) (2019) 309–319, https://doi.org/10.1111/ppl.12928.
[73] M.S. Bray, T.K. Lenz, J.C. Bowman, A.S. Petrov, A.R. Reddi, N.V. Hud, L.D. Williams, J.B. Glass, Ferrous Iron Folds rRNA and Mediates Translation, 2018, https://doi.org/10.1101/256958 bioRxiv 256958.
[74] P. Rodríguez-Lucena, L. Hernández-Apaolaza, J.J. Lucena, Comparison of iron chelates and complexes supplied as foliar sprays and in nutrient solution to correct iron chlorosis of soybean, J. Plant Nutr. Soil Sci. 173 (1) (2010) 120–126, https://doi.org/10.1002/jpln.200800256.
[75] C.M. Ferreira, C.A. Sousa, I. Sanchis-Pérez, S. López-Rayo, M.T. Barros, H.M. Soares, J.J. Lucena, Calcareous soil interactions of the iron (III) chelates of DPH and Azotochelin and its application on amending iron chlorosis in soybean (Glycine max), Sci. Total Environ. 647 (2019) 1586–1593, https://doi.org/10.1016/j.scitotenv.2018.08.069.
[76] I. Bajalan, M. Zand, S. Rezaee, Allelopathic effect of various organs of walnuts (Juglans regia) on seed germination of wheat, Amer.-Eur. J. Agric. Environ. Sci. 13 (9) (2013) 1293–1297.
[77] A. Alyousef, G. Ibrahim, Inhibitory effect of fruit hull and leaves of pistachio on weed growth in pots, Internat. J. Pharm. Tech. Res. 7 (2) (2014) 365–369.